## CHAPTER 19

# HIGHER ORDER WAVE SPECTRA[1]

By Paul C. Liu[2], M. ASCE and Albert W. Green[3]

## 1. INTRODUCTION

As part of an effort aimed at examining the empirical aspects of nonlinear processes of wind-generated waves, this paper presents calculations and examples of bispectra and trispectra and indicates applications of these results to the study of wave growth processes.

Recent publications on wave studies have indicated that the growth process of wind waves is primarily associated with the nonlinear energy flux due to wave-wave interactions. While most of these studies are conjectures from theoretical considerations, it is of interest to explore the nonlinear studies empirically. From available wave data largely recorded at a single station, a first step is to perform bispectral and trispectral analyses of the data. Since the unispectrum provides information on the energy content of the frequency components, the bispectrum and trispectrum generally provide information on the interactive relations between two and three frequency components, respectively. These higher order interactive relations can thus be considered as estimates or characterizations of nonlinear interactions.

Hasselmann, Munk, and McDonald (1962), perhaps the first to use bispectral analysis, demonstrated that calculations of observed bispectra of ocean waves correlate reasonably well with theoretically derived bispectra. Other ocean wave bispectra were presented by Garrett (1970) and Houmb (1974). Trispectral analysis has not yet been attempted in practical problems.

## 2. CALCULATION PROCEDURES

By definition, a bispectrum is the two-dimensional Fourier transform of the third-order covariance function of the data; a trispectrum is the three-dimensional Fourier transform of the fourth-order covariance function of the data. A two- or three-dimensional Fourier transform of the corresponding covariance function is generally cumbersome

---

[1] GLERL Contribution No. 160.

[2] Physical Scientist, Physical Limnology and Meteorology Group, Great Lakes Environmental Research Laboratory, National Oceanic and Atmospheric Administration, 2300 Washtenaw Avenue, Ann Arbor, Michigan 48104.

[3] Chief, Physical Oceanography Branch, Oceanography Division, Naval Oceanographic Research and Development Activity, Code 331, NSTL Station, Mississippi 39529.

to calculate. However, following procedures discussed by Haubrich (1965) and Hinch and Clay (1968), which use fast Fourier transform directly on the data, the bispectrum and trispectrum can be feasibly calculated.

For a given discrete series of $\ell$ data points at a sampling interval $\Delta t$, $\zeta(\ell\Delta t)$, with $\ell = 1, 2, \ldots, L$, subdividing the series into P non-overlapping subseries, each of length K, such that $p = 0, 1, \ldots, p - 1$ and $k = 1, 2, \ldots, K$ yield

$$\zeta_p(k\Delta t) = \zeta[(pK + k)\Delta t],$$

and the K complex Fourier efficients for each group are given by

$$X_p(\omega) = \left(\frac{\Delta t}{2\pi K}\right)^{1/2} \sum_{j=1}^{K} \zeta_p(j\Delta t)e^{i2\pi kj/K} \quad , \quad k = 1, 2, \ldots, K. \tag{1}$$

Then the unispectrum, the bispectrum, and the trispectrum can be estimated by

$$S_2(\omega) = \frac{1}{P} \sum_{p=1}^{P} X_p(\omega)X_p^*(\omega) \quad , \tag{2}$$

$$S_3(\omega_1,\omega_2) = \frac{1}{P} \sum_{p=1}^{P} X_p(\omega_1)X_p(\omega_2)X_p^*(\omega_1 + \omega_2) \quad , \tag{3}$$

and

$$S_4(\omega_1,\omega_2,\omega_3) = \frac{1}{P} \sum_{p=1}^{P} X_p(\omega_1)X_p(\omega_2)X_p(\omega_3)X_p^*(\omega_1 + \omega_2 + \omega_3) \quad , \tag{4}$$

respectively. The asterisks in equations (2)-(4) indicate complex conjugates. In the actual computations P = 30 is used for each 20-min data segment of L = 1800 and $\Delta t = 2/3$ s to obtain smoothed spectral estimates with 60 degrees of freedom.

Because of the symmetric relations in the definitions of higher order spectra, spectral estimates are needed only within a fundamental region. The fundamental region for $S_2(\omega)$ is the line segment $0 \le \omega \le \omega_N$; for $S_3(\omega,\omega_1)$ the triangle defined by $0 \le \omega \le \omega_1$ and $0 \le \omega_1 \le \omega_N$; and for $S_4(\omega,\omega_1,\omega_2)$ the tetrahedron defined by $0 \le \omega \le \omega_1$, $0 \le \omega_1 \le \omega_2$, and $0 \le \omega_2 \le \omega_N$, with $\omega_N = 2\pi/(2\Delta t)$ representing the Nyquist frequency. A detailed discussion of these procedures and their theoretical backgrounds is given in Liu (1977a).

## 3. HIGHER ORDER SPECTRA OF KNOWN FUNCTIONS

In order to understand and interpret the higher order spectral behavior of actual wave data, unispectra, bispectra, and trispectra of three known functions are first calculated as examples. Figures 1, 2, and 3 show the results for a synthesized sinusoidal record with three frequency components, a Gaussian white noise, and a second-order autoregressive process, respectively. All calculations are based on 1800 generated data points at 2/3-s sampling intervals.

In the figures, logarithms of unispectral density are plotted versus frequency; the bispectra show the contours of the logarithms of bispectral amplitude plotted in the triangular fundamental region. The increasing contour levels are represented by the increasing darkness in the shaded areas. For the trispectra, a tetrahedral fundamental region is represented by cutting discrete layers along one frequency axis parallel to the plane formed by the other two frequency axes. In each trispectral layer, the number on the corner represents the third frequency. The logarithms of trispectral amplitude are again contoured, with increasing level represented by increasing darkness in the shaded areas.

Figure 1 shows the sinusoidal wave with three frequency components of 0.1 Hz, 0.2 Hz, and 0.3 Hz. There are three delta functions at the three components in the unispectrum. Its bispectrum has strong interactions at components (0.1, 0.1), (0.2, 0.2), (0.3, 0.3), as well as (0.1, 0.2), (0.1, 0.3), and (0.2, 0.3). Its trispectrum is characterized by the strong interactions between the various second-order interactions shown in the bispectrum and other frequency components, with the strongest interaction at (0.1, 0.1, 0.1), (0.2, 0.2, 0.2), and (0.3, 0.3, 0.3).

Figure 2 shows the results for the computer-generated Gaussian white noise. Its bispectrum is practically zero and its trispectrum is characterized by random patterns without specifically stronger interactions. Figure 3 shows the second-order autoregressive process $X_t$ defined by

$$X_t = X_{t-1} - 0.5X_{t-2} + Z_t \quad ,$$

where $Z_t$ is the Gaussian white noise generated for Figure 2. Its unispectrum, bispectrum, and trispectrum are all characterized by higher interactions at the low frequency range and a gradual decrease in magnitude toward the higher frequencies.

It is clearly shown by these results that bispectral and trispectral densities are directly related to and dependent on unispectral characteristics, which is what would be expected from theoretical analysis (Hasselmann, 1962). It seems reasonable to infer that the higher order interactions presented in this paper are estimates of nonlinear interactions.

As the basic assumption for higher order spectral analysis is stationarity while the growth process of surface waves is clearly nonstationary, a modified assumption of local stationarity in which the

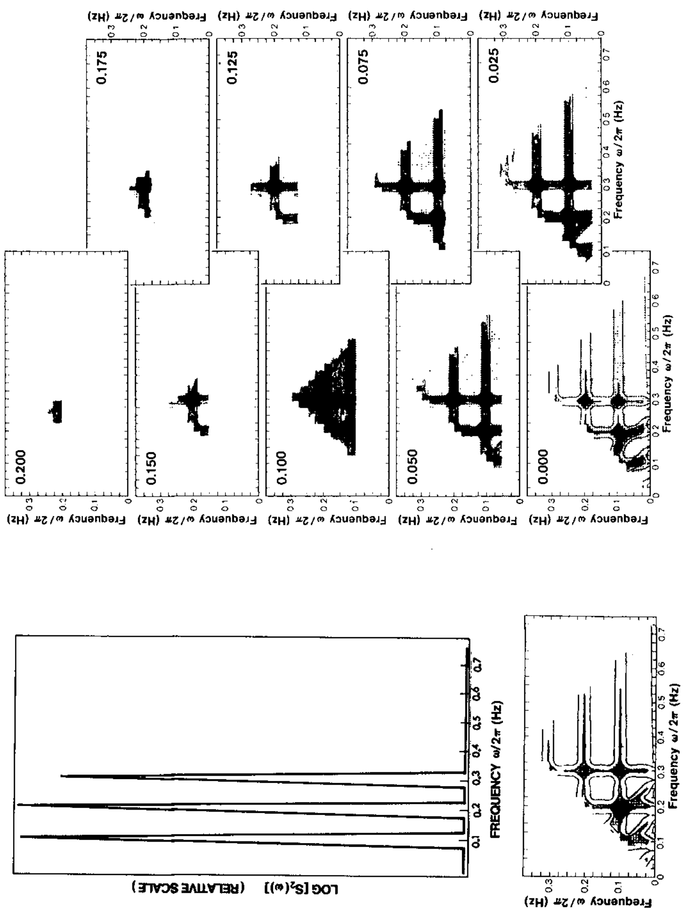


Figure 1 Spectra for a sinusoidal wave with three frequency components.

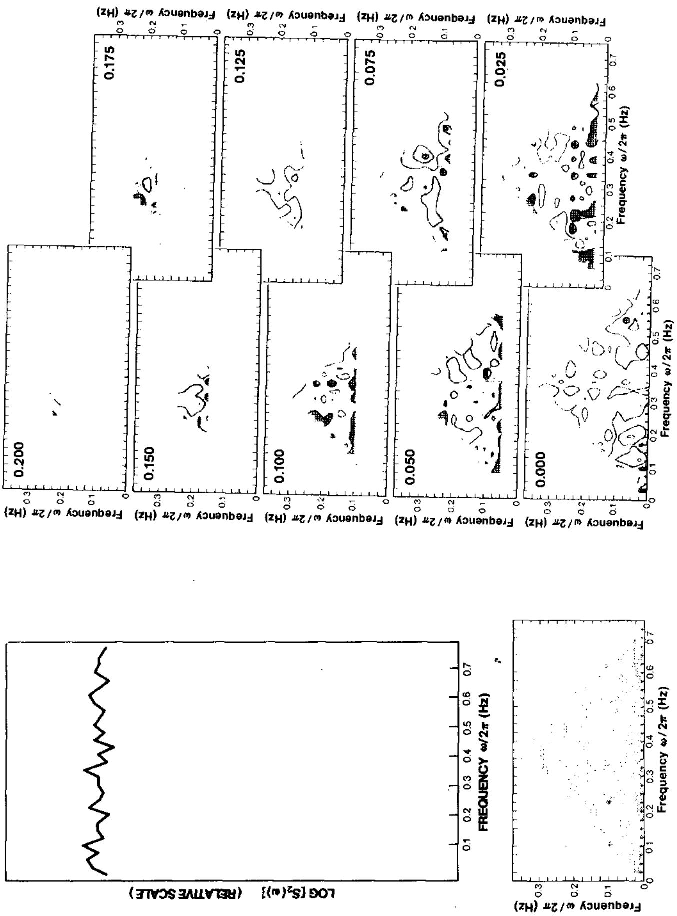


Figure 2 Spectra for a Gaussian white noise.

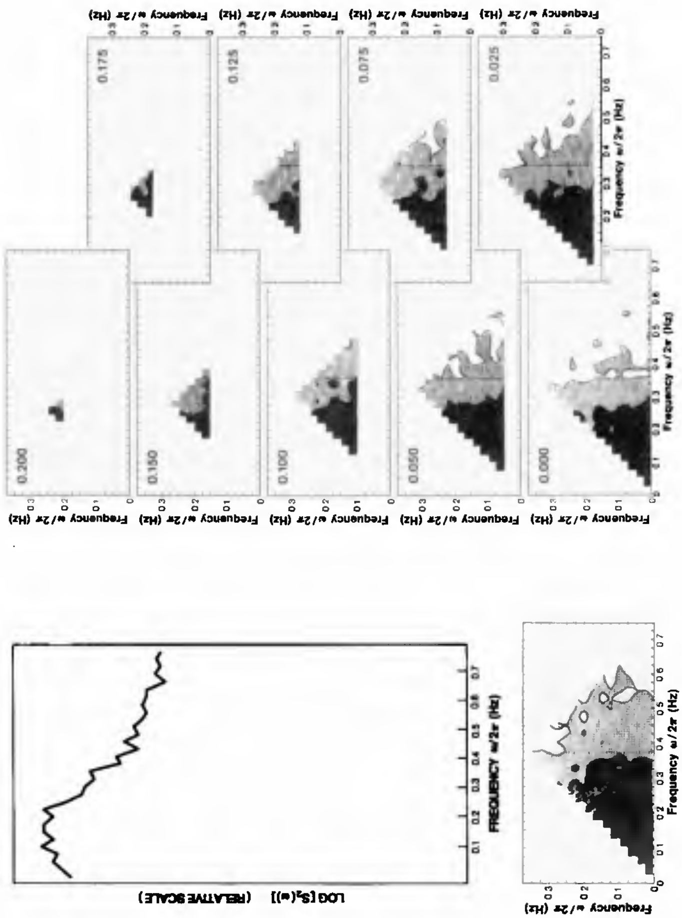


Figure 3 Spectra for a second-order autoregressive process.

process is considered to be stationary only within a local time interval can be used. A previous study (Liu, 1977b) indicated that the local stationarity assumption is statistically acceptable in actual applications.

## 4. HIGHER ORDER SPECTRA OF WAVE DATA

The calculations using equations (1)-(4) have been applied to an episode of recorded wave data. The episode was recorded continuously on 9 August 1972 in Lake Ontario approximately 35-km offshore of Oswego, New York, with a Waverider deployed in 150 m of water. Figure 4 shows the wind conditions during the episode, which started at a wind speed of 8 m $s^{-1}$ and increased to over 11 m $s^{-1}$ in 3 hours. The westerly wind direction provided fairly constant and long fetches during the episode. The group of short straight lines plotted on the figure indicates the locations in time of 64 overlapping segments of wave data analyzed for the episode. Each segment is 20-min long and has a 17.5-min overlap with the next segment. Figure 5 shows the computed unispectral density versus frequency versus time. The three-dimensional perspective figure presents a clear overview of spectral growth during the episode. Figure 6 presents six bispectra from the episode at 30-min intervals as representative of the whole process. As the temporal variations are gradual, the figures clearly show that the magnitude of the bispectral amplitude increases and the hills and ridges migrate toward lower frequencies during wave growth. Figure 7 presents three representative trispectra at 1-hour intervals. The trispectrum on the left is 2.5 min from the beginning of the episode; the one in the middle is 1-hour later, with the trispectral interactions increasing and migrating toward lower frequencies; the one on the right is 2 hours from the first during the intensive wave growth stage. The intensity of trispectral density has increased significantly as shown by the very dark contour areas.

These results give only qualitative features of the higher order spectra during wave growth. In order to use these results for quantitative study, efforts must be made to examine the relative growth behavior of the individual higher order spectral components. Liu (1977a) has pursued this approach and found that, during the intensive stage of wave growth, the interaction between the components of peak-energy frequency and the next lower frequency grows consistently stronger than its interaction with the next higher frequency. Thus, the peak-energy frequency transfers more energy to the lower frequency components than to the higher ones, confirming the well-known fact that unispectral peaks shift progressively toward lower frequencies during wave growth.

## 5. CONCLUDING REMARKS

This paper has presented results of higher order wave spectra calculations with an intent to study nonlinear processes of wave growth by examining these higher order interactions. While the higher order spectra can be feasibly calculated from given wave data, it is only

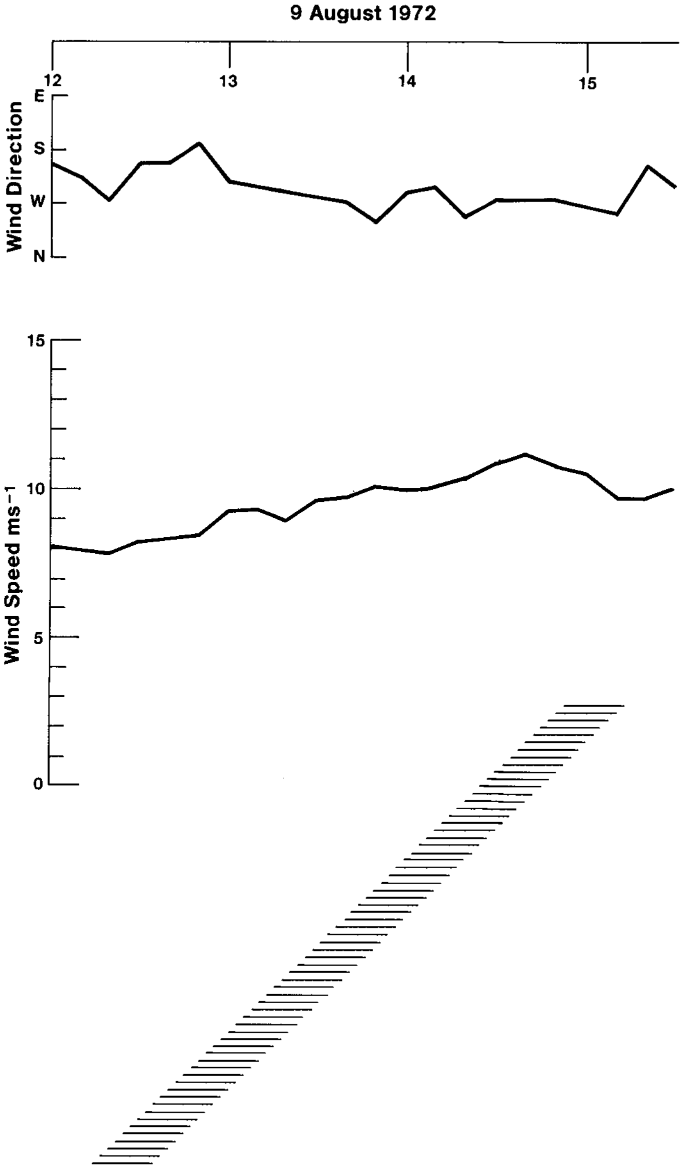


Figure 4 Wind conditions for the 9 August 1972 episode in eastern Lake Ontario.

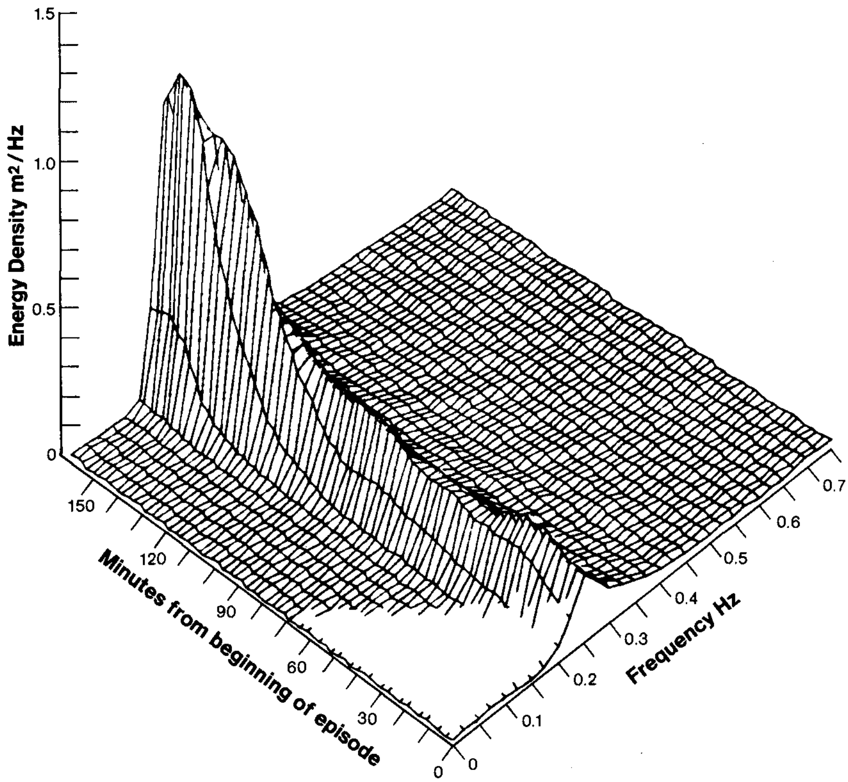


Figure 5 Perspective view of unispectra versus time during the 9 August 1972 episode.

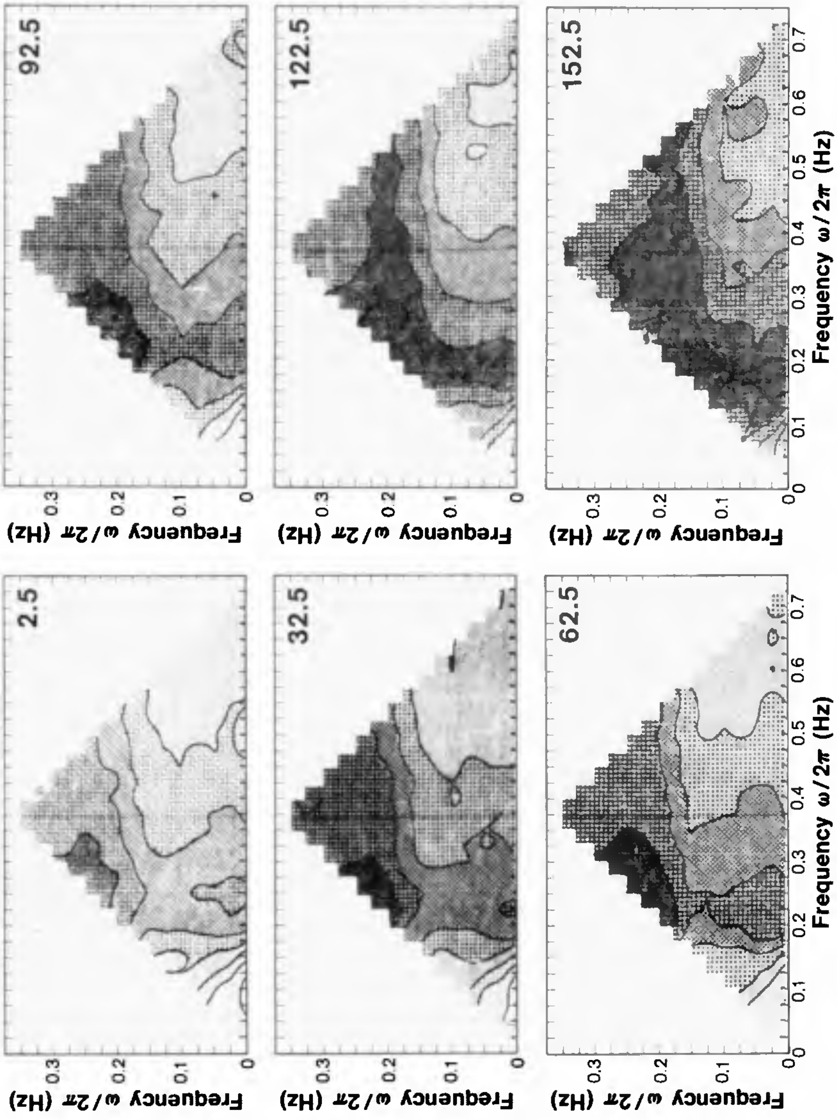


Figure 6 Bispectra during the 9 August 1972 episode. The numbers 2.5, 32.5, . . . , and 152.5 represent minutes from beginning of the episode.

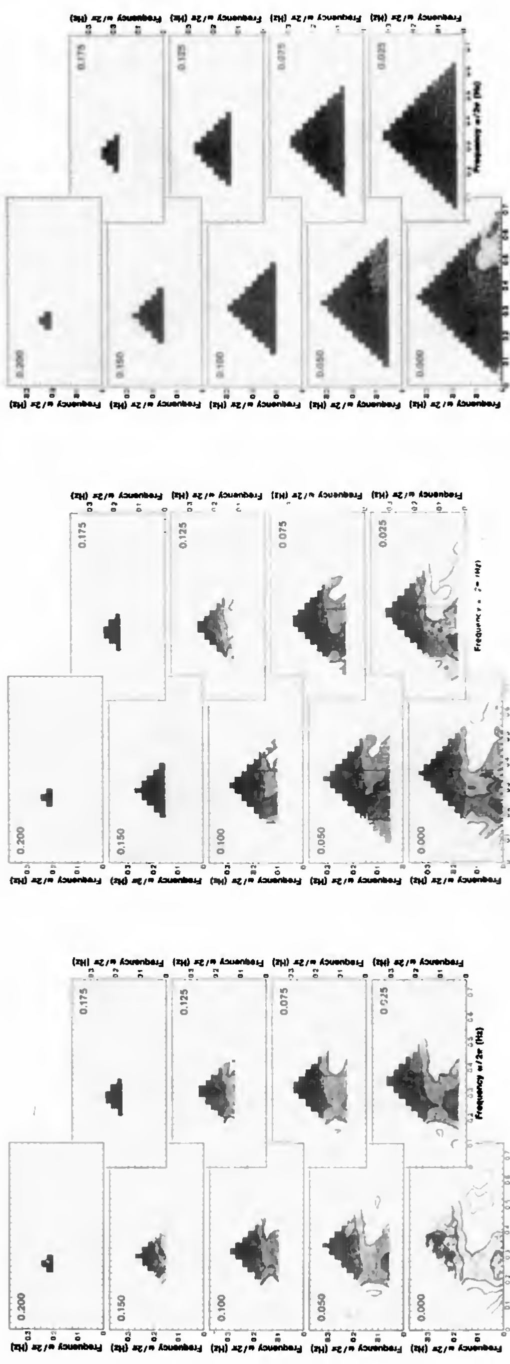

Figure 7 Trispectra during the 9 August 1972 episode at 1 hour interval from left.

inferred that these spectra are estimates of nonlinear interactions. At present, nonlinear processes have only been studied theoretically; it is hoped that an empirical effort presented in this paper will serve to indicate another approach to greater understanding of the processes. Efforts to further interpret and use these results will be continued.

## 6. REFERENCES

Garrett, J. F. (1970): Field observations of frequency domain statistics and nonlinear effects in wind-generated ocean waves. Ph.D. Thesis, the University of British Columbia.

Hasselmann, K. (1962): On the nonlinear energy transfer in a gravity-wave spectrum. Part 1: General theory. *J. Fluid Mech.*, 12:481-500.

Hasselmann, K., W. Munk, and G. McDonald (1962): Bispectra of ocean waves. In: *Time Series Analysis*, Ed. M. Rosenblatt, Wiley, New York, 125-139.

Haubrich, R. A. (1965): Earth noise, 5 to 500 millicycles per second. Part 1, Spectral stationarity, normality, and nonlinearity. *J. Geophys. Res.*, 70:1415-1427.

Hinch, M. J., and C. S. Clay (1968): The application of the discrete Fourier transform in the estimation of power spectra, coherence, and bispectra of geophysical data. *Rev. Geophys. Space Phys.*, 6:347-363.

Houmb, O. G. (1974): Spectra and bispectra of ocean waves. In: *Proc. 14th Coastal Engineering Conf.*, Vol. 1, American Society of Civil Engineers, Copenhagen, Denmark, 301-320.

Liu, P. C. (1977a): Temporal spectral growth and nonlinear characteristics of wind waves in Lake Ontario. Ph.D. Thesis, the University of Michigan.

Liu, P. C. (1977b): Higher order spectra and stationarity of wind waves. In: *Preprint Proceedings of the Fifth Conference on Probability and Statistics*, American Meteorological Society, Las Vegas, Nevada, 254-259.